

## PAPER

[View Article Online](#)  
[View Journal](#) | [View Issue](#)Cite this: *RSC Sustainability*, 2025, 3, 1149

# Exploiting rice industry wastewater for more sustainable sunlight-driven photocatalytic hydrogen production using a graphitic carbon nitride polymorph†

Petra Bianchini,<sup>a</sup> Antonella Profumo,<sup>a</sup> Lorenzo Cerri,<sup>b</sup> Costanza Tedesco,<sup>a</sup> Lorenzo Malavasi <sup>a</sup> and Andrea Speltini <sup>\*a</sup>

This paper shows the results collected in lab-scale experiments for photocatalytic H<sub>2</sub> evolution from rice industry wastewater, by using a cheap and eco-friendly graphitic carbon nitride catalyst, one-pot prepared by the sacrificial template method. The final effluent from the production of “rice milk” beverage proved to be really rewarding compared to pure water, highlighting the possibility of taking advantage of a sugar-rich matrix to boost H<sub>2</sub> formation. After preliminary experiments in glucose aqueous solution, yielding a maximum gas evolution above 1000 μmoles g<sup>−1</sup> h<sup>−1</sup>, the study moved on to wastewater and the operational conditions were optimized through designed experiments, under simulated solar light. Production of about 150 μmoles g<sup>−1</sup> h<sup>−1</sup>, at least 380-fold greater than production from neat water, was achieved by working with just 0.5 g L<sup>−1</sup> of catalyst directly in the raw effluent, thus limiting the amount of metal co-catalyst and avoiding sample dilution. The reproducibility of the process was good, with relative standard deviations below 12% (*n* = 3). The production was also verified under natural sunlight, obtaining a mean production of nearby 115 μmoles g<sup>−1</sup> h<sup>−1</sup>. The sustainability of this photocatalytic setup is strengthened by the recyclability of the catalyst, which maintains its photoactivity for at least four treatments.

Received 12th September 2024  
Accepted 9th February 2025

DOI: 10.1039/d4su00567h

[rsc.li/rscsus](https://rsc.li/rscsus)

## Sustainability spotlight

The search for new ways to retrieve clean energy is a priority for satisfying the increase in energy demand while avoiding the adverse effects of fossil fuels on the environment. H<sub>2</sub>, the most appealing clean energy vector, can be generated from water through photocatalysis, exploiting sunlight. This work combines such elements to achieve greener H<sub>2</sub> directly from rice industry wastewater, an abundant waste produced worldwide. The convenience of using raw effluent with a small amount of catalyst, the recyclability of the catalyst and the effectiveness of the process under sunlight were demonstrated. This study is in line with the Affordable and clean energy (SDG7) and the Climate action (SDG 13) goals of the UN 2030 Agenda for Sustainable Development.

## Introduction

Urbanization, industrialization and population growth have led, in the last few decades, to great consumption of non-renewable energy; hence the search for new alternative sources is now in the spotlight.<sup>1–3</sup> In this context, hydrogen is very attractive due to its high specific heat, low density and lack of secondary pollution.<sup>2,3</sup> H<sub>2</sub> can be obtained through different pathways, but presently most gas is generated using fossil fuels or by electrolysis of water using electricity that is, however, largely derived from fossil fuels. Thus, this is a not sustainable

and environmentally benign practice. An alternative method is using water and electrical energy obtained from renewable sources or water and solar light as the driving force, thus achieving a really clean gas, regarded as “green” hydrogen.<sup>4</sup> In this framework, photocatalysis plays a prominent, emerging role to produce hydrogen from water and biomass under mild conditions,<sup>1,5</sup> but it still needs safe, recyclable, and efficient catalysts with enlarged visible light harvesting and charge carrier separation, as an alternative to titanium dioxide, the most extensively studied semiconductor.<sup>6</sup>

In recent years, polymeric organic semiconductor graphitic carbon nitride (g-C<sub>3</sub>N<sub>4</sub>) has emerged as an eco-friendly catalyst, and nowadays it is one of the most promising photocatalysts for H<sub>2</sub> production, CO<sub>2</sub> reduction, N<sub>2</sub> fixation, and C–C bond formation.<sup>7,8</sup> Its attractiveness lies in its facile synthesis from cheap precursors, extended light absorption in the visible region of the solar spectrum, and high thermal and chemical

<sup>a</sup>Department of Chemistry, University of Pavia, via Taramelli 12, 27100 Pavia, Italy.  
E-mail: [andrea.speltini@unipv.it](mailto:andrea.speltini@unipv.it)

<sup>b</sup>Riso Scotti S.p.A., via Scotti 2, 27100 Pavia, Italy

† Electronic supplementary information (ESI) available. See DOI: <https://doi.org/10.1039/d4su00567h>

stability.<sup>7–9</sup>  $g\text{-C}_3\text{N}_4$  is a 2D material characterized by a bulk, disordered graphitic structure, but it suffers from two main drawbacks: the high recombination rate of the charge carriers and low surface area. To overcome these limitations, heterojunction engineering with other semiconductors has been the most investigated route for the first problem, while surface treatments, such as laser ablation, ultrasonication or sacrificial template methods, address the second problem.<sup>7,10,11</sup> Using KCl as a sacrificial template in the synthesis, the formation of poly(heptazine imide), PHI, a  $g\text{-C}_3\text{N}_4$  polymorph with similar optical properties to the bulk material but increased crystallinity and photoactivity, was proved.<sup>10–12</sup>

Despite this, in the modern literature the use of PHI has been documented for cellulose photoreforming,<sup>13</sup> and hydrogen peroxide production<sup>14</sup> but not for hydrogen evolution from wastewater. Indeed, in the green  $\text{H}_2$  economy, efforts should be undertaken to pursue the concept of sustainability, which meets another cornerstone of sustainable development, that is the circular economy.

To date, research on photocatalytic  $\text{H}_2$  production has been only partially directed to the recovery of wastewater,<sup>6,15</sup> which could be a resource owing to residual oxidizable compounds being used as sacrificial agents to boost  $\text{H}_2$  evolution.<sup>15,16</sup> Nevertheless, to date some pioneering studies have provided evidence for the concrete possibility of valorising waste to retrieve hydrogen gas.<sup>15–24</sup> In particular, simulated wastewaters were tested using  $\text{MoS}_2$  quantum dots-decorated  $\text{ZnIn}_2\text{S}_4$  combined with reduced graphene oxide,<sup>16</sup> and a platinized  $\text{H}_2\text{WO}_4/\text{TiO}_2$  S-scheme heterojunction.<sup>24</sup> Other studies were conducted on real effluents employing different catalysts, namely sulfide wastewater from biogas production using  $\text{Cu}_2\text{-S@TiO}_2$  core-shell composites,<sup>22</sup> olive mill wastewater with conventional  $\text{Pt/TiO}_2$ ,<sup>18</sup> biodiesel wastewater using  $\text{Pd/TiO}_2$ ,<sup>23</sup> refinery sulfide wastewater with cerium-doped  $\text{TiO}_2$ ,<sup>19</sup> effluent from a plant producing fruit juice with  $\text{Au/TiO}_2$ ,<sup>20</sup> and brewery wastewater using graphitic carbon nitride ( $g\text{-C}_3\text{N}_4$ ) catalysts.<sup>15,21</sup> A recent overview of photocatalytic hydrogen production, including water splitting and biomass/waste valorisation, provides evidence of the importance of this research area.<sup>25</sup>

Based on such a background, the novelty of the present work is the evaluation of rice industry wastewater to obtain  $\text{H}_2$  *via* photocatalysis through a last-generation catalyst, *viz.* a poly(heptazine imide) material prepared by a single-step synthesis from low-cost precursors. In particular, the final effluent from the production of so-called “rice milk”, provided by the Italian company Riso Scotti S.p.A., was considered in view of its large-scale production and residual content of saccharides, mainly glucose, valuable as sacrificial agents to sustain  $\text{H}_2$  production from water.<sup>6,15</sup> This food product, more properly described as a rice drink due to its vegetal origin, is particularly rich in saccharides ( $40\text{--}80\text{ g L}^{-1}$ ) derived from starch during the maceration of rice in water in the presence of enzymes. This is a two-phase enzymatic digestion involving dextrinization and saccharification, promoted by  $\alpha$  amylase and glucoamylase, respectively. Briefly, rice, water, and the enzymes are put into a reaction for the transformation of starches into dextrins, and dextrins into sugars. Once the extraction process has taken

place, the drink is homogenized with rice oil to improve palatability and cooled. Through a decanter, the fibres are separated from the drink, which is then sterilized and packaged in cartons. The Riso Scotti S.p.A. division that is in charge of the production of “rice milk” and other beverages, uses approximately  $800\text{ m}^3$  of water per day and generates approximately  $650\text{ m}^3$  of wastewater every day; thus seeking possible ways to utilize this high-volume production waste is relevant for the vision of a circular economy.

The process was first studied in a standard aqueous solution of glucose as a model sacrificial biomass, then in the industrial wastewater. The best conditions were established through a chemometric study and then the performance of the system was compared to that of commercial titanium dioxide, as the conventional benchmark semiconductor. Further experiments were conducted under natural solar light, and the possibility of recovering the catalyst for consecutive photocatalytic treatments was also investigated.

## Experimental

### Chemicals and materials

$\text{H}_2\text{PtCl}_6$  (38% Pt basis), KCl (99%) and melamine (99%) and sleeve stopper septa were purchased from Merck (Milan, Italy). Evonik AEROXIDE® P25  $\text{TiO}_2$  (77.1% anatase, 15.9% rutile, 7% amorphous  $\text{TiO}_2$ , particle size 10–50 nm, surface area  $60.8\text{ m}^2\text{ g}^{-1}$ ) was purchased from Evonik Industries AG (Hanau, Germany). Glucose (99.9%) was supplied by Carlo Erba Reagents (Milan, Italy) and  $0.45\text{ }\mu\text{m}$  nylon membranes were obtained from Scharlab Italia S.r.l. (Lodi, Italy). Pyrex® photoreactors (single-neck cylindrical vessels,  $\varnothing$  4 cm, h 2 cm, 28 mL capacity) were manufactured by Tecnovetro (Monza, Italy). Industrial wastewater was provided by Riso Scotti S.p.A. (Pavia, Italy). Four final effluent samples deriving from the operations of clean-in-place washing, water lubrication of pumps, homogenizers and packaging lines, and the aseptic barrier on the sterilization lines, were merged to give a laboratory pool that was divided into 100 mL-aliquots, and stored at  $-20\text{ }^\circ\text{C}$  until use (physical-chemical parameters are shown in Table S1†).

### Synthesis and characterization of the catalyst

$g\text{-C}_3\text{N}_4$  in the form of PHI phase was synthesized using KCl as a sacrificial template by the polycondensation of melamine (MLM). Through the exploitation of KCl as a sacrificial water-soluble template, the formation was proved of poly(heptazine imide), PHI, a  $g\text{-C}_3\text{N}_4$  polymorph that shows similar optical properties to  $g\text{-C}_3\text{N}_4$  but higher crystallinity and increased photoactivity than  $g\text{-C}_3\text{N}_4$ .<sup>26</sup> Based on the HER from aqueous triethanolamine and on the synthesis reaction yield,<sup>26</sup> the KCl : MLM 20 : 1 molar ratio appeared to be the most convenient and, accordingly, was selected here. Briefly, the metal halide was previously dried at  $100\text{ }^\circ\text{C}$  for 24 h and then the photocatalyst was synthesized in a tubular oven at  $550\text{ }^\circ\text{C}$  under  $\text{N}_2$  flow for 4 h ( $1\text{ }^\circ\text{C min}^{-1}$  heating rate). The as-obtained yellowish powder was sonicated in deionized water for 1 h, then repeatedly washed to eliminate the residual KCl, filtered, and dried at  $60\text{ }^\circ\text{C}$  overnight.



The PHI was characterized by X-ray diffraction (XRD), scanning electron microscopy (SEM), transmission electron microscopy (TEM), UV-vis diffuse reflectance spectroscopy (DRS), and Brunauer–Emmett–Teller (BET) surface area measurements (for details, see ESI†).

### Photocatalytic experiments

H<sub>2</sub> evolution was studied in distilled water containing glucose and in rice industry wastewater (21 mL), irradiated in glass containers. After adding the catalyst, a small volume of an aqueous solution of H<sub>2</sub>PtCl<sub>6</sub>, used as a metal co-catalyst precursor, was added to the sample. Metallic Pt was formed *in situ* from photoreduction of the precursor metal ions on the catalyst surface during irradiation, according to the photo-deposition method.<sup>27–29</sup> After degassing by Ar bubbling (20 min), the photoreactor was closed with a sleeve stopper septum and subjected to irradiation (4 h, magnetic stirring) under simulated solar light (500 W m<sup>−2</sup>, BST control temperature 65 °C) in a Solar Box 1500e (CO.FO.ME.GRA S.r.l., Milan, Italy) equipped with a UV outdoor filter made of IR-treated soda lime glass. The apparent photon flux was  $1.53 \times 10^{-7}$  photon moles per s; under the best conditions, the apparent quantum yield (AQY%) was calculated as the percent ratio ( $2 \times$  H<sub>2</sub> moles)/incident photon moles,<sup>6</sup> and the turnover number (TON) as the ratio H<sub>2</sub> moles/Pt moles.<sup>27</sup>

Experiments under natural sunlight were performed on a window ledge in Pavia (45°11'46" N, 9°09'38" E, 77 m altitude) on a sunny summer's day (11 am–3 pm, 5 July 2024); the solar power, measured by HD 9221 (Delta OHM) (450–950 nm) and multimeter (CO.FO.ME.GRA) (295–400 nm) pyranometers, ranged from 478 to 500 W m<sup>−2</sup> in the visible range, and between 25.6 and 27.2 W m<sup>−2</sup> in the UV region. The global radiation ranged from 580 to 900 W m<sup>−2</sup> while temperature varied between 26 °C and 28 °C.

For catalyst recycling, the powder was recovered (0.45 µm filtration) and washed with distilled water before reuse.

All analytical determinations are described in ESI.† The H<sub>2</sub> production data are hereafter reported as micromoles of gas per gram of catalyst per hour (µmoles g<sup>−1</sup> h<sup>−1</sup>, HER). Reproducibility was evaluated based on the RSD% from independent photoproduction tests.

## Results and discussion

### Catalyst characterization

Fig. 1 shows the structural characterization of the photocatalyst through XRD. The formation of PHI exploiting KCl as the template during MLM polymerization has already been shown in previous reports.<sup>13,14,30</sup> The pattern exhibits few evident peaks, the strongest being at 28.2°, which is referenced to the (001) crystal plane.

The optical characterization of the photocatalytic material is reported in Fig. 2.

The UV-vis absorption spectrum confirms, in agreement with the literature,<sup>12,26</sup> an absorption edge of about 460 nm, and a band gap value of 2.7 eV, as calculated from the Tauc plot.

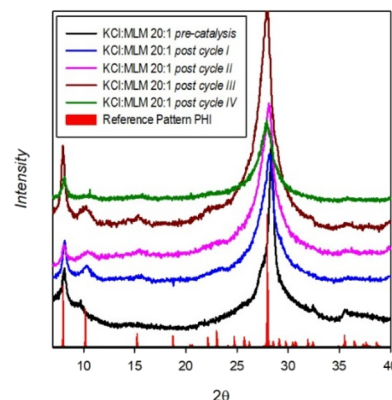


Fig. 1 XRD patterns of the as-obtained PHI (black line), after the first photocatalytic cycle (blue line), after two photocatalytic cycles (pink line), after three photocatalytic cycles (dark red line), after four photocatalytic cycles (green line), and the reference pattern of PHI (red line).

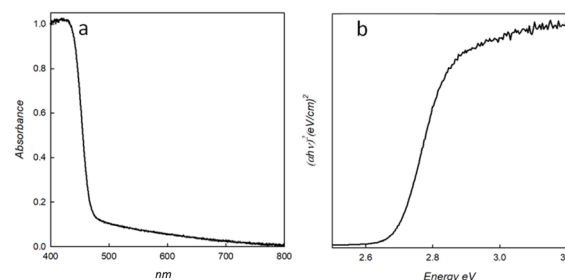


Fig. 2 UV-vis absorption spectrum (a) and Tauc plot (b) acquired for the PHI sample.

The morphology and microstructure of PHI, investigated by TEM and SEM, are displayed in Fig. 3. It is apparent that the PHI sample exhibits an exfoliated sheet structure with the presence of small particles and large reduction of the thickness of the layer, as evident from the light colour of the TEM image.

From the BET measurements it was verified that the PHI semiconductor has a surface area very close to that of the bulk, 15.5 m<sup>2</sup> g<sup>−1</sup> and 17.5 m<sup>2</sup> g<sup>−1</sup>, respectively, and this may suggest that the higher HER of PHI, previously evaluated in standard tests,<sup>26</sup> is imputable mainly to the increased density of active sites in the modified photocatalyst together with the improvement in optical response.<sup>26</sup>

### Photocatalytic H<sub>2</sub> production

The study was carried out on the g-C<sub>3</sub>N<sub>4</sub> material (PHI) that resulted in a high-performance catalyst for H<sub>2</sub> production from triethanolamine aqueous solution, coupled to Pt as the metal co-catalyst, as discussed in a recent study by this research group.<sup>26</sup>

This catalyst, very appealing in being prepared from cheap precursors through a simple one-pot procedure, and showing greater visible light absorption than titanium dioxide,<sup>6</sup> was here evaluated to move towards more sustainable H<sub>2</sub> production



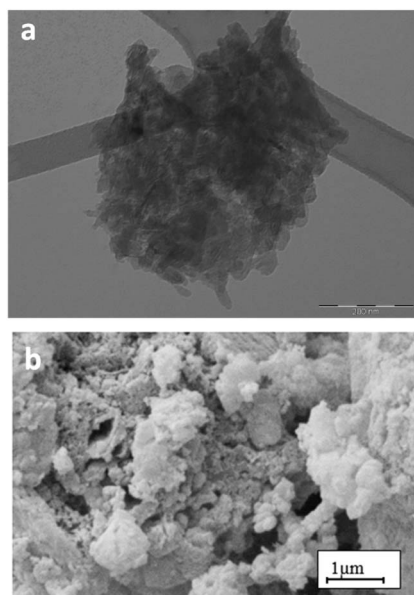


Fig. 3 TEM (a) and SEM (b) images of the PHI sample.

from aqueous biomass, which was optimized by a multivariate approach. With this aim, in the first part of the work a series of lab-scale experiments was planned in water containing glucose,<sup>20</sup> chosen as a representative biomass-derived sacrificial agent, considering that different food industry wastewaters contain up to tens of grams per litre of residual sugars.<sup>20,21</sup> This has become relevant, as bio-oxygenated compounds for H<sub>2</sub> photoproduction are now counted as alternative resources to meet energy needs.<sup>31</sup>

A full 2<sup>3</sup> design of experiments (DoE) was accomplished following the experimental domain reported in Table S2,<sup>†</sup> where the variables involved in the photocatalytic process, namely glucose concentration ( $x_1$ ), catalyst concentration ( $x_2$ ) and co-catalyst loading ( $x_3$ ), are studied at two levels (low and high). The responses, experimentally obtained as mean HER from duplicate experiments (Table S3<sup>†</sup>), were modelled using CAT software (Chemometric Agile Tool),<sup>32</sup> which provided the plot of the coefficients of the model together with the response surfaces, as shown in the ESI (Fig. S1 and S2),<sup>†</sup> as the output of the elaboration. It was found that the biomass concentration was the most influential factor ( $**p < 0.01$ ), with the highest level favouring the reaction, probably due to the facilitated mass transfer of the solute to the catalytic surface.<sup>27,33</sup> The same is true for the high level of co-catalyst, although to a lesser extent ( $*p < 0.05$ ), but combined with the lowest amount of catalyst ( $**p < 0.01$  for their interaction). The production peak, above 1000  $\mu\text{moles g}^{-1} \text{h}^{-1}$  for the model monosaccharide, is competitive compared to previous studies on aqueous glucose treated under UV or solar radiation in the presence of metal-decorated g-C<sub>3</sub>N<sub>4</sub> (ref. 21 and 34) or TiO<sub>2</sub> (ref. 35 and 36) semiconductors, and it highlights the potential of this PHI photoactive material.

Driven by these outcomes, we then moved on to the processing water from the production of so-called “rice milk”. The

first trials were carried out in duplicate both on the sample as-received and after 1 : 4 v/v dilution to reduce the apparent opalescence of the waste, which can hamper light penetration during irradiation. Under these conditions (1 g per L of catalyst, 0.5 wt% Pt), gas formation was low (around 5  $\mu\text{moles g}^{-1} \text{h}^{-1}$ ) in the raw sample, but significantly higher compared to deionized water (<0.4  $\mu\text{moles g}^{-1} \text{h}^{-1}$ , not quantifiable), which was tested as the control. Only traces of H<sub>2</sub> (<0.4  $\mu\text{moles g}^{-1} \text{h}^{-1}$ ) were found from the diluted matrix, suggesting that a smaller dilution factor could be considered.

These preliminary results prompted us to further investigate the possibility of recycling this waste. Another DoE was set up and experiments were carried out, based on the experimental domain shown in Table 1.

To evaluate the possible effect of the amount of biomass (quantified as glucose), the wastewater was used after 1 : 2 v/v dilution (low level) or as-received (high level).

The HERs achieved according to the experimental plan are reported in Table S4,<sup>†</sup> while the plot of the coefficients of the model is shown in Fig. 4.

As can be seen, the first and second variables significantly affect the process. In particular, the HER is improved by avoiding waste dilution ( $x_1$ , high level) and using 0.5 g L<sup>-1</sup> as the catalyst concentration ( $x_2$ , low level). Moreover, the  $x_2x_3$  coefficient indicates that the interaction between catalyst amount and Pt loading is significant; in particular, when using the lowest concentration of catalyst, the highest value is required

Table 1 Experimental domain for the 2<sup>3</sup> factorial design

	Levels	
	−1	+1
Waste dilution (v/v), $x_1$	1 : 2	None
Catalyst concentration (g L <sup>-1</sup> ), $x_2$	0.5	2
Pt loading (wt%), $x_3$	0.5	3

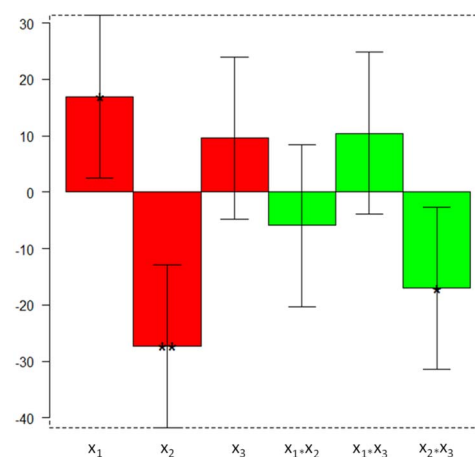


Fig. 4 Plot of the coefficients of the model where the stars indicate the significance of the coefficients ( $*p < 0.05$ ,  $**p < 0.01$ ,  $***p < 0.001$ ), while error bars indicate the confidence intervals ( $p = 0.05$ ).





for the co-catalyst. In any case, the amount of metal deposited on the g-C<sub>3</sub>N<sub>4</sub> surface is strongly mitigated by the low concentration of the catalyst, and by its durability for multiple photo-reactions (see later in the text).

The response surfaces (Fig. 5) graphically show the role of the variables relative to their interactions in terms of H<sub>2</sub> produced (y-axis).

The model, elaborated on the experimental data is given in eqn (1):

$$\text{HER} = 54 + 17x_1 - 27x_2 + 10x_3 - 6x_1x_2 + 10x_1x_3 - 17x_2x_3 \quad (1)$$

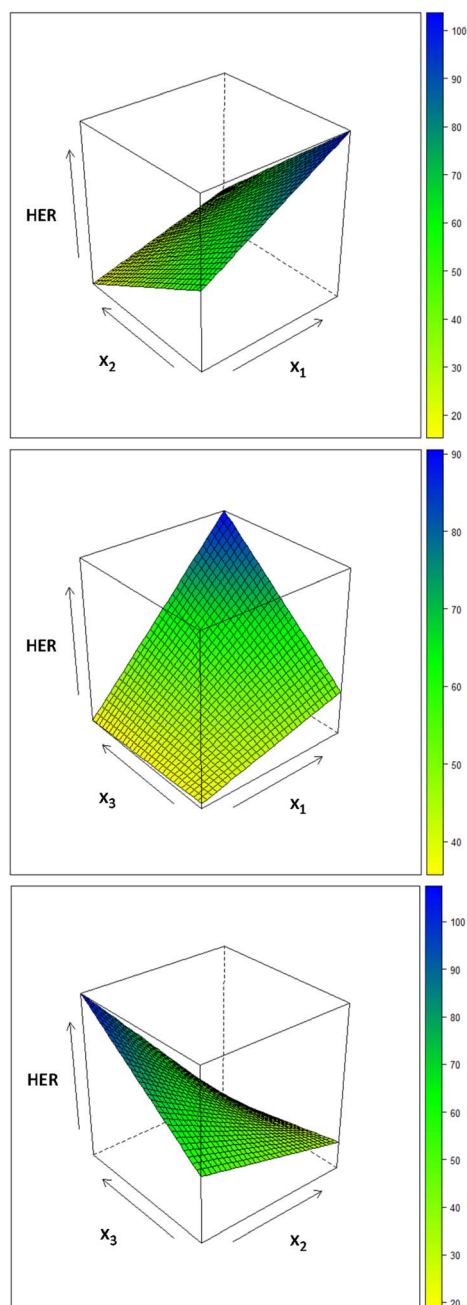


Fig. 5 Response surfaces obtained by CAT from the experimental results of H<sub>2</sub> production from the wastewater.

The chemometric study clearly indicates that the best conditions are: no waste dilution, 0.5 g per L catalyst, 3 wt% Pt. This conclusion was confirmed at the test point [ $x_1 = 0$ ;  $x_2 = 0$ ;  $x_3 = 0$ ], which means 1 : 1 v/v dilution, 1.25 g per L catalyst, 1.75 wt% Pt, obtaining an HER of  $53 \pm 6 \mu\text{moles g}^{-1} \text{ h}^{-1}$  ( $p = 0.05$ ,  $n = 4$ ). The experimental datum is not statistically different from the value predicted by the model (see eqn (1)), viz.  $54 \mu\text{moles g}^{-1} \text{ h}^{-1}$ ; therefore the model is validated.

The maximum production, *i.e.*  $148 \mu\text{moles g}^{-1} \text{ h}^{-1}$ , corresponds to a TON of around 4, with an AQY about 0.65% higher than the data collected on brewery and dairy wastewaters using oxidized g-C<sub>3</sub>N<sub>4</sub> (coupled with Pt) as an alternative to commercial titanium dioxide.<sup>21</sup> In terms of H<sub>2</sub> produced, recycling this type of effluent is rewarding, as is apparent by comparing its HER to that observed under sunlight in other wastewaters rich in saccharides using TiO<sub>2</sub> coupled with Au<sup>20</sup> or modified g-C<sub>3</sub>N<sub>4</sub> coupled with Pt.<sup>21</sup>

Although deep insight into the reaction mechanism is beyond the scope of the present study, the central role of the biomass in the wastewater was ascertained from the same experiments performed in pure water (distilled water) that yielded an HER at least 380 times lower, with the evolved H<sub>2</sub> being negligible ( $<0.4 \mu\text{moles g}^{-1} \text{ h}^{-1}$ ), as the contribution from “direct” water splitting.<sup>37</sup> This is clear evidence of the action of the residual saccharides in the industrial waste as sacrificial electron donors<sup>6,38</sup> in sustaining gas formation through photo-reforming, also referred to as “sacrificial water splitting”,<sup>37</sup> supporting the recovery of this waste for energy retrieval. Conversely, H<sub>2</sub> was not detected ( $<0.003 \mu\text{moles h}^{-1}$ ) either in the dark or without PHI, as expected, maintaining the same amount of metal co-catalyst in the sample solution (both under light and in darkness), thereby confirming the photocatalytic pathway that underlies the reaction and the role of the PHI catalyst. On the other hand, the gas formation below  $0.4 \mu\text{moles g}^{-1} \text{ h}^{-1}$  observed in Pt-free irradiation experiments, with PHI alone, confirms both the action of the co-catalyst and the synergistic effect that takes place when the metal is coupled with the graphitic carbon nitride polymorph, providing  $148 \mu\text{moles g}^{-1} \text{ h}^{-1}$  (the highest HER achieved under the best conditions).

The composition of the liquid phase after photocatalysis was investigated by liquid chromatography (Table S5†). With regard to the organic fraction, the reduction of the glucose concentration (around 90%) proves the transformation of the sugars during treatment, which was also confirmed by the identification of furfural and hydroxymethylfurfural, investigated as key byproducts, in the solution, at concentrations of  $41 \mu\text{g L}^{-1}$  and  $13 \mu\text{g L}^{-1}$ , respectively, while methylfurfural was not detectable. Since formic acid was present after the reaction but was also in the original sample, as determined by ion chromatography, it is reasonable to assume that the final concentration derives from both processes of sugar oxidation and conversion of formic acid in solution to carbon dioxide by dehydrogenation.<sup>28,31</sup> Indeed, CO<sub>2</sub> was found in the gas phase ( $122 \mu\text{moles g}^{-1} \text{ h}^{-1}$ ), but CO was not detectable. Given these experimental data and based on previous studies on H<sub>2</sub> production from aqueous phase saccharides over platinized catalysts,<sup>21,27,39–41</sup> we can



hypothesize a mechanism that combines sugar oxidation with water splitting under anaerobic conditions, called biomass photoreforming,<sup>28</sup> in which (1) the catalyst absorbs the radiation that generates the typical charge separation (holes and electrons); (2) the sacrificial electron donor organic compounds act as scavenger of oxidizing species and supplies electrons and protons by undergoing oxidative photoreforming;<sup>39,40,42</sup> (3) the metal acts as an electron collector to enhance biomass photoreforming, also sustaining hydrogen ion reduction, while preventing charge carrier recombination.<sup>27,40,43,44</sup>

The HER obtained was satisfactorily compared to experiments done using historical P25 TiO<sub>2</sub>. The latter was tested in the effluent under the conditions previously reported for standard saccharide solutions,<sup>21</sup> observing a mean HER of 638  $\mu\text{moles g}^{-1} \text{h}^{-1}$ , possibly attributable to its higher surface area.<sup>45</sup>

Overall, the performance of the system is attractive as the HER is similar to or even higher than those attained in other food industry streams,<sup>20,21</sup> with a remarkably more eco-friendly g-C<sub>3</sub>N<sub>4</sub> catalyst that does not require any post-synthesis treatment.<sup>21,46</sup>

After the optimization of the photocatalytic system, the subsequent part of the work was addressed to assessing the sustainability of the process. The latter is definitely improved when stable and recyclable photoactive materials are available.<sup>47</sup> Recycling tests in the effluent under the best conditions – simply washing the recovered powder with water – provided evidence for the long-term stability of g-C<sub>3</sub>N<sub>4</sub> (Fig. 6). Indeed, it was used four times with almost unchanged photocatalytic activity (Fig. 6), with just a 24% decrease at the fourth use.

These findings are supported by the XRD spectrum of the spent catalyst (Fig. 1, green line) compared to the pattern of the fresh one (Fig. 1, black line). The main peaks of the PHI phase at 8°, 10° and 27° are still clearly visible after four photocatalytic cycles, and this could justify the retention of the PHI performance. However, progressive peak broadening and a reduction in the relative intensity of the main peaks as a function of the number of reuse cycles indicate a slight loss of PHI crystallinity, possibly due to the repeated exploitation of the catalyst, but which does not significantly influence the HER. However, we

cannot exclude possible catalyst fouling caused by the lipid component<sup>18</sup> derived from the rice oil used as an additive in the beverage production.

To demonstrate the feasibility of carrying out the photoreaction under natural solar light, irradiation experiments were done on a window ledge under natural illumination (outdoor conditions), during the central hours of the day. The mean HER was 114  $\mu\text{moles g}^{-1} \text{h}^{-1}$  under the real conditions described in the experimental section, with good reproducibility (RSD < 12%,  $n = 4$ ). This value is in good agreement with that measured, 130  $\mu\text{moles g}^{-1} \text{h}^{-1}$ , under simulated conditions in solar box (800 W m<sup>-2</sup>, 35 °C). These results point towards a solar-driven H<sub>2</sub>-evolving system, to be assessed in future studies at the pilot plant scale.<sup>38,39</sup>

## Conclusions

This study shows the potential of wastewater produced at large scale worldwide by the agri-food sector for obtaining clean energy in the form of molecular hydrogen *via* photocatalysis. The latter proved to be a safe and smart approach, as it combined in the same system solar light, wastewater and a low-cost, eco-friendly catalyst. The optimization of the experimental conditions through the multivariate approach allowed H<sub>2</sub> evolution from the rice industry waste to be maximized, achieving far higher production than that from pure water. The valorisation of this effluent, the possibility of working under natural solar light with a low amount of catalyst, and its photostability and reusability are major goals in the field of sustainable energy.

## Data availability

The data supporting this article have been included as part of the ESI.†

## Author contributions

PB: investigation, software, visualization, writing – review & editing; AP: writing – review & editing, validation, funding acquisition; LC: resources, writing – review & editing; CT: investigation; writing – review & editing; LM: conceptualization, resources; AS: writing – original draft, writing – review & editing, conceptualization, project administrator, funding acquisition; supervision.

## Conflicts of interest

There are no conflicts to declare.

## Acknowledgements

This research was in the framework of the “PON Ricerca e Innovazione” PhD project of Petra Bianchini, DOT1322889-10, D. M. 10-08-2021, no. 1061, supported by “Ministero dell'Università e della Ricerca (MUR)” and the European Union. The Authors also acknowledge the support of “Ministero

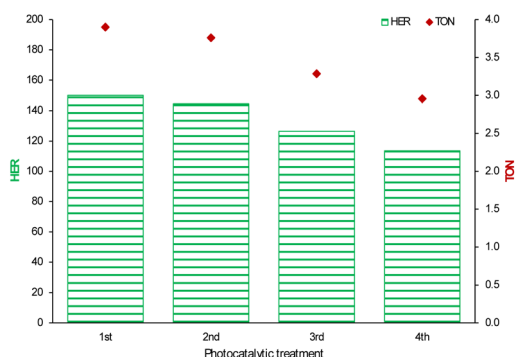


Fig. 6 Reusability of the g-C<sub>3</sub>N<sub>4</sub> catalyst in raw wastewater under simulated solar light ( $n = 2$ ): HER (y-axis on the left), TON (y-axis on the right).



dell'Università e della Ricerca (MUR)" and the University of Pavia through the program "Dipartimenti di Eccellenza 2023–2027". LabAnalysis srl (Casanova Lonati, Pavia, Italy) is acknowledged for the HPLC-MS analysis.

## References

- 1 Y. Huang, J. Xie, J. Zhang and Y. Pan, *J. Mol. Struct.*, 2024, **1307**, 138043.
- 2 X. Jing, Y. Zhang, H. Chang, R. Qiu, W. Yang, H. Xie, W. Wang, M. Zhang, X. Lyu, Q. Liu, X. Wang, J. Crittenden and X. Lyu, *J. Environ. Chem. Eng.*, 2024, **12**, 113040.
- 3 Z. Wang, M. Dou, X. Liu, S. Kang, L. Kong, H. Yang, Y. Zhang, Y. Chen, H. Zhu and J. Dou, *J. Environ. Chem. Eng.*, 2024, **12**, 113080.
- 4 A. Abboto, *Idrogeno Tutti I Colori Dell'energia*, Edizioni Dedalo, Bari (Italy), 2020.
- 5 H. A. Maitlo, B. Anand and K. H. Kim, *Appl. Energy*, 2024, **361**, 122932.
- 6 S. S. Mani, S. Rajendran, T. Mathew and C. S. Gopinath, *Energy Adv.*, 2024, **3**, 1472–1504.
- 7 M. Shalom, S. Inal, C. Fettkenhauer, D. Neher and M. Antonietti, *J. Am. Chem. Soc.*, 2013, **135**, 7118–7121.
- 8 E. I. García-López, L. Palmisano and G. Marci, *Chem. Eng.*, 2023, **7**, 11.
- 9 M. Ismael, Q. Shang, J. Yue and M. Wark, *Mater. Today Sustainability*, 2024, **27**, 100827.
- 10 K. Schwinghammer, B. Tuffy, M. B. Mesch, E. Wirnhier, C. Martineau, F. Taulelle, W. Schnick, J. Senker and B. V. Lotsch, *Angew. Chem., Int. Ed.*, 2013, **52**, 2435–2439.
- 11 K. Li, L. Bao, S. Cao, Y. Xue, S. Yan and H. Gao, *ACS Appl. Energy Mater.*, 2021, **4**, 12965–12973.
- 12 T. Xiong, W. Cen, Y. Zhang and F. Dong, *ACS Catal.*, 2016, **6**, 2462–2472.
- 13 D. B. Nimbalkar, V.-C. Nguyen, C.-Y. Shih and H. Teng, *Appl. Catal., B*, 2022, **316**, 121601.
- 14 I. Krivtsov, A. Vazirani, D. Mitoraj, M. M. Elnagar, C. Neumann, A. Turchanin, Y. Patiño, S. Ordóñez, R. Leiter, M. Lindén, U. Kaiser and R. Beranek, *J. Mater. Chem. A*, 2023, **11**, 2314–2325.
- 15 G. Li, X. Deng, P. Chen, X. Wang, J. Ma, F. Liu and S.-F. Yin, *Chem. Eng. J.*, 2022, **433**, 134505.
- 16 S. Zhang, L. Wang, C. Liu, J. Luo, J. Crittenden, X. Liu, T. Cai, J. Yuan, Y. Pei and Y. Liu, *Water Res.*, 2017, **121**, 11–19.
- 17 M. I. Badawy, M. Y. Ghaly and M. E. M. Ali, *Desalination*, 2011, **267**, 250–255.
- 18 A. Speltini, M. Sturini, F. Maraschi, D. Dondi, G. Fisogni, E. Annovazzi, A. Profumo and A. Buttafava, *Int. J. Hydrogen Energy*, 2015, **40**, 4303–4310.
- 19 J. Bharatvaj, V. Preethi and S. Kanmani, *Int. J. Hydrogen Energy*, 2018, **43**, 3935–3945.
- 20 M. Imizcoz and A. V. Puga, *Catalysts*, 2019, **9**, 584.
- 21 A. Speltini, F. Gualco, F. Maraschi, M. Sturini, D. Dondi, L. Malavasi and A. Profumo, *Int. J. Hydrogen Energy*, 2019, **44**, 4072–4078.
- 22 V. Navakoteswara Rao, N. Lakshmana Reddy, M. Mamatha Kumari, P. Ravi, M. Sathish, K. M. Kuruvilla, V. Preethi, K. Raghava Reddy, N. P. Shetti, T. M. Aminabhavi and M. V. Shankar, *Appl. Catal., B*, 2019, **254**, 174–185.
- 23 N. Jandam, K. Serivalsatit, M. Hunsom and K. Pruksathorn, *ACS Omega*, 2021, **6**, 24709–24719.
- 24 G. Dong, T. Zhou, W. Wei, X. Ding, Q. Tang, W. Shi, T. Zeng, L. Gui and Y. Chen, *Int. J. Hydrogen Energy*, 2024, **60**, 1309–1316.
- 25 *Photocatalytic Hydrogen Production for Sustainable Energy*, ed. A. Puga, Wiley-VCH GmbH, 2023, online ISBN: 978-352783542-3, print ISBN: 978-352734983-8, DOI: [10.1002/9783527835423](https://doi.org/10.1002/9783527835423).
- 26 M. Medina-Llamas, E. Bianchi, M. C. Mozzati, C. Tedesco, C. Milanese, A. Speltini, A. Profumo, V. Armenise, A. Milella, A. Listorti and L. Malavasi, *ChemSusChem*, 2025, **18**, e202400918.
- 27 A. Speltini, L. Romani, D. Dondi, L. Malavasi and A. Profumo, *Catalysts*, 2020, **10**, 1259.
- 28 A. V. Puga, *Coord. Chem. Rev.*, 2016, **315**, 1–66.
- 29 J. H. Zhang, M. J. Wei, Z. W. Wei, M. Pan and C. Y. Su, *ACS Appl. Nano Mater.*, 2020, **3**, 1010–1018.
- 30 A. Jin, Y. Jia, C. Chen, X. Liu, J. Jiang, X. Chen and F. Zhang, *J. Phys. Chem. C*, 2017, **121**, 21497–21509.
- 31 J. Kennedy, H. Bahruji, M. Bowker, P. R. Davies, E. Bouleghlimat and S. Issarapanacheewin, *J. Photochem. Photobiol., A*, 2018, **356**, 451–456.
- 32 R. Leardi, C. Melzi and G. Polotti, CAT, chemometric agile tool, freely downloadable from <http://gruppochemiometria.it/index.php/software>, 2019, accessed July 2024.
- 33 P. Gomathisankar, D. Yamamoto, H. Katsumata, T. Suzuki and S. Kaneco, *Int. J. Hydrogen Energy*, 2013, **38**, 5517–5524.
- 34 F. Ding, H. Yu, W. Liu, X. Zeng, S. Li, L. Chen, B. Li, J. Guo and C. Wu, *Mater. Des.*, 2024, **238**, 112678.
- 35 M. Bellardita, E. I. García-López, G. Marci, G. Nasillo and L. Palmisano, *Eur. J. Inorg. Chem.*, 2018, **2018**, 4522–4532.
- 36 P. Tkachenko, V. Volchek, A. Kurenkova, E. Gerasimov, P. Popovetskiy, I. Asanov, I. Yushina, E. Kozlova and D. Vasilchenko, *Int. J. Hydrogen Energy*, 2023, **48**, 23366–23378.
- 37 M. Bowker, *Catal. Lett.*, 2012, **142**, 923–929.
- 38 M. I. Maldonado, A. López-Martín, G. Colón, J. Peral, J. I. Martínez-Costa and S. Malato, *Appl. Catal., B*, 2018, **229**, 15–23.
- 39 K. Villa, X. Domènech, S. Malato, M. I. Maldonado and J. Peral, *Int. J. Hydrogen Energy*, 2013, **38**, 12718–12724.
- 40 A. Speltini, M. Sturini, D. Dondi, E. Annovazzi, F. Maraschi, V. Caratto, A. Profumo and A. Buttafava, *Photochem. Photobiol. Sci.*, 2014, **13**, 1410–1419.
- 41 A. Speltini, A. Scalabrini, F. Maraschi, M. Sturini, A. Pisanu, L. Malavasi and A. Profumo, *Int. J. Hydrogen Energy*, 2018, **43**, 14925–14933.
- 42 A. Rioja-Cabanillas, D. Valdesueiro, P. Fernández-Ibáñez and J. A. Byrne, *J. Phys. Energy*, 2021, **3**, 012006.
- 43 D. Y. C. Leung, X. Fu, C. Wang, M. Ni, M. K. H. Leung, X. Wang and X. Fu, *ChemSusChem*, 2010, **3**, 681–694.



- 44 L. I. Granone, D. W. Bahnemann, F. Sieland, N. Zheng, R. Dillert and D. W. Bahnemann, *Green Chem.*, 2018, **20**, 1169–1192.
- 45 X. Jiang, M. Manawan, T. Feng, R. Qian, T. Zhao, G. Zhou, F. Kong, Q. Wang, S. Dai and J. H. Pan, *Catal. Today*, 2018, **300**, 12–17.
- 46 A. Pisanu, A. Speltini, B. Vigani, F. Ferrari, M. Mannini, N. Calisi, B. Cortigiani, A. Caneschi, P. Quadrelli, A. Profumo and L. Malavasi, *Dalton Trans.*, 2018, **47**, 6772–6778.
- 47 X. Liang, J. Liu, H. Guo, H. Li, E. Liu, Y. Zhao, Y. Ji and J. Fan, *J. Environ. Chem. Eng.*, 2023, **11**, 109987.

